Observing volcanic signatures from space, and in the lab

A. J. A. Smith, E. Carboni, D. M. Peters, G. E. Thomas, T. M. Sears, A. Dudhia, R. G. Grainger
Atmospheric, Oceanic and Planetary Physics, University of Oxford.
smith@atm.ox.ac.uk

Abstract

The Earth Observation Data Group at the University of Oxford has a wide range of tools that can be applied to the observation of volcanic ash.

Lab measurements of volcanic ash from the Aso, Eyjafjallajökull, and Tongariro eruptions have provided size distribution, extinction, and refractive index data which are then used to create forward models of volcanic ash plumes for satellite aerosol retrievals.

Using visible and near infra-red measurements from SEVIRI, AATSR and MODIS, the ORAC optimal estimation retrieval can provide optical depth, effective radius, aerosol speciation, and (with AATSR) plume height.

In the infra-red, IASI and MIPAS fast flagging methods, relying on unique features of the IR volcanic ash spectrum, can be used to spot potential danger areas for aircraft in real time. An IASI SO_2 retrieval providing plume height and column concentration is also available, and is used along with the above ash flags and retrievals to discuss the merits of using SO_2 flagging as a proxy for areas likely to contain volcanic ash.

Measuring volcanic ash refractive index

Ash aerosol refractive index can be derived from transmission measurements in the near IR. Here, an example using ash taken from the 1993 eruption of Mt Aso, Japan is used. The sample was sieved to $< 22.5\,\mu$m, resuspended, and introduced into an aerosol test cell with optical windows. Spectral intensity measurements through the test cell were taken using a Bruker IFS-66 FTS at the Rutherford Appleton Laboratory Molecular Spectroscopy Facility. Measurements were obtained with and without the aerosol to calculate the transmission spectrum, $T(\lambda)$.

Aerosol cell transmission relates to the physical properties of the aerosol via Bouguer's Law ($T(\lambda) = e^{-\beta_{\text{ext}}(\lambda)\,x}$) where β_{ext} is the volume extinction coefficient at wavelength λ, and x the path length though the test cell. Assuming a light scattering model (e.g. Mie theory for spherical particles) and knowing the particle size distribution allows the extinction coefficient to be calculated from

$$\beta_{\text{ext}}(\lambda) = \int_0^\infty Q_{\text{ext}}(r,\lambda)\,\pi r^2\,n(r)\,dr,$$

where Q_{ext} is the extinction efficiency, r is the particle radius, and $n(r)\,dr$ is the number of particles with radii between r and $r + dr$. The complex refractive index wavelength dependence $m(\lambda)$ is represented by a damped harmonic oscillator model to reduce the number of model parameters to less than the number of measured spectral points. Optimal estimation is then used to derive the band model parameters (and hence refractive index, see Fig. 1) and aerosol size distribution. The method is described in detail by Thomas et al. [2005].

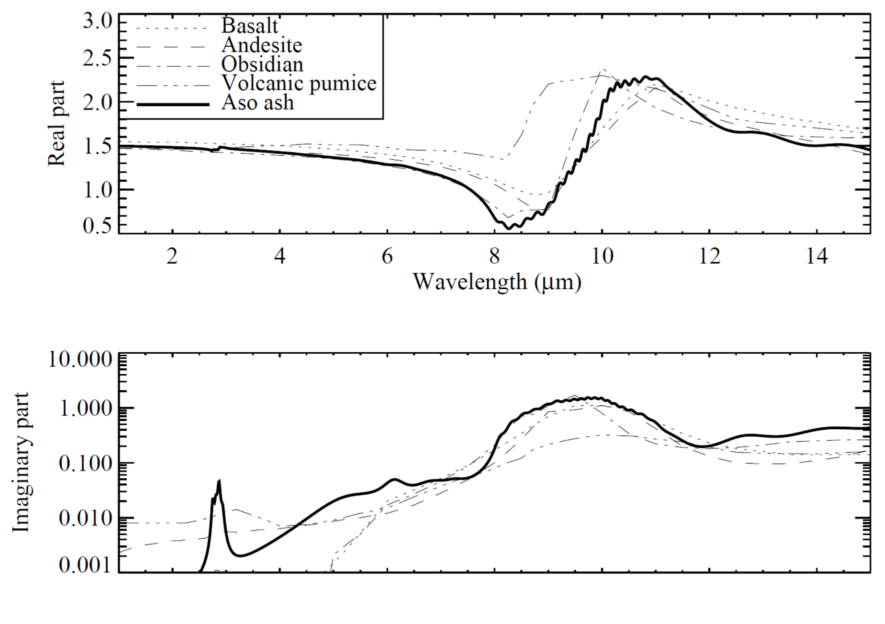

Fig. 1: Real and imaginary refractive index components, determined from a sample of ash from the 1993 eruption of Mt Aso, Japan. The refractive indices of basalt, andesite, obsidian and volcanic pumice are also shown.

The ORAC aerosol retrieval

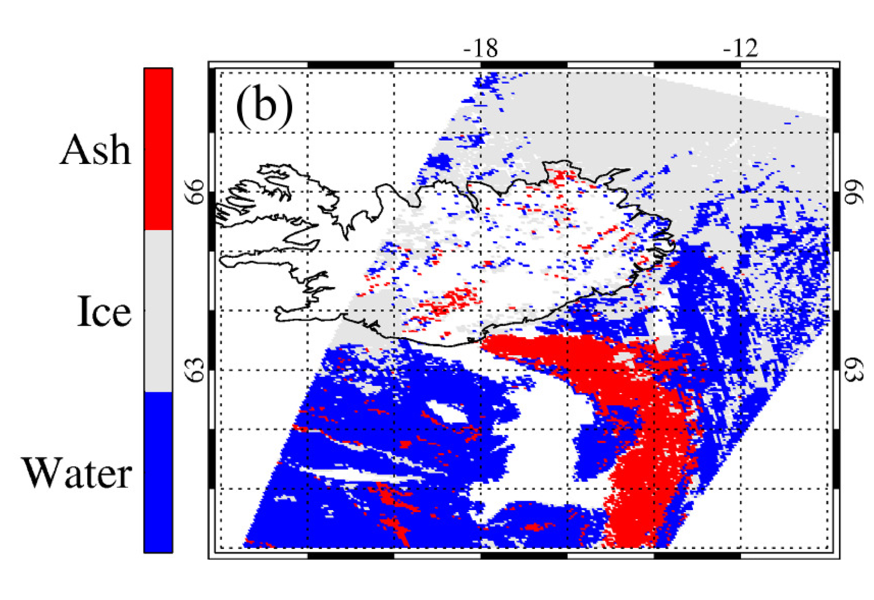

Fig. 2: The ORAC best-fitting cloud type for images acquired by AATSR at 12.13 GMT on 6th May 2010.

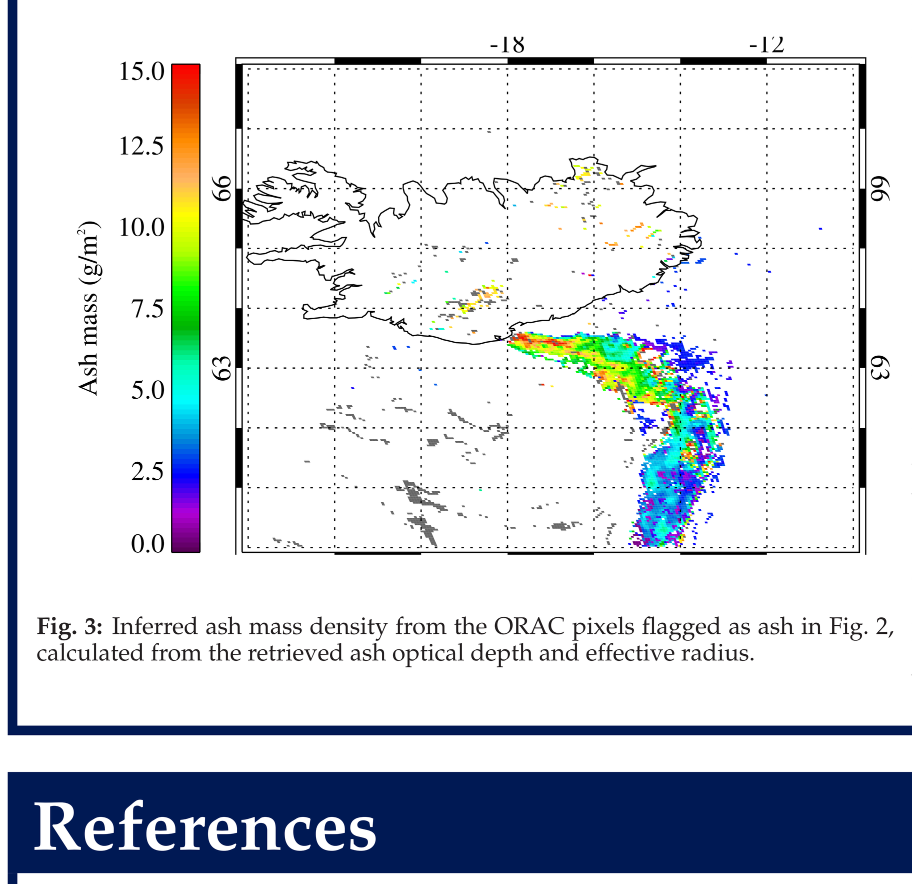

Fig. 3: Inferred ash mass density from the ORAC pixels flagged as ash in Fig. 2, calculated from the retrieved ash optical depth and effective radius.

The Oxford-RAL Aerosol and Cloud (ORAC) optimal estimation retrieval [Poulsen et al., 2012] can be applied to the retrieval of volcanic ash cloud properties. Using assumed optical properties of volcanic ash in the visible and infrared, the retrieval produces estimates of the location of the ash, its height, optical depth and radius. Figure 2 shows the cloud type which produced the best fit to the ORAC observations of the Eyjafjallajökull plume captured by the Advanced Along Track Scanning Radiometer (AATSR) on the 6th May 2010, Figure 3 shows an estimate of the column ash mass concentration derived from the retrieved optical depth and radius.

The retrieval is dependant on prior knowledge of the ash optical properties and is subject to significant errors when the ash lies over lower level water clouds. However it is hoped that its performance can be improved by incorporating a dual-layer cloud forward model. Aerosol altitude can also be obtained by either adding additional thermal channels, or by using the AATSR dual views to obtain the height by parallax.

Flagging volcanic ash with IASI

Ash flagging uses a methodology based on that of Walker et al. [2011] and Carboni et al. [2012], designed to detect trace gases in IASI data. The principle idea is to use a generalised error covariance that contains not only the instrument noise, but covariance due to interfering trace gases and broadband scatterers (such as aerosols and clouds) that should be unrelated to the required retrieved property. Since these signals are included in the covariance, they need not be retrieved or their variance taken account of in the forward model of the atmosphere.

A proxy optical depth is retrieved by linearisation about some background level, τ_0, so that a least squares estimate of τ can be obtained by

$$\tau = \tau_0 + \left(\mathbf{K}^T\mathbf{S}_\epsilon^{-1}\mathbf{K}\right)^{-1}\mathbf{K}^T\mathbf{S}_\epsilon^{-1}\,(\mathbf{y} - \bar{\mathbf{y}})\,.$$

where $\mathbf{y}$ is a measurement, and $\mathbf{K}$ is the Jacobian of the measurement with respect to optical depth $\frac{\partial \mathbf{y}}{\partial \tau}$. The error covariance matrix, $\mathbf{S}_\epsilon$, is built up from IASI measurements in the days preceeding the eruption and in the same geographical area (so that it contains the variation for this location, and time of year, but no volcanic covariance).

Proxy optical depth values are not accurate, but for cases where there is no volcanic signal, they lie very close to τ_0. Volcanic signals stand out above the noise by several standard deviations and can be flagged as being of suspected volcanic origin.

Fig. 4 shows comparisons of τ, brightness temperature difference (BTD) between 11 and 12 μm, and column SO_2 (described below). Ash and SO_2 plumes match well, but the BTD method shows issues over bright surfaces.

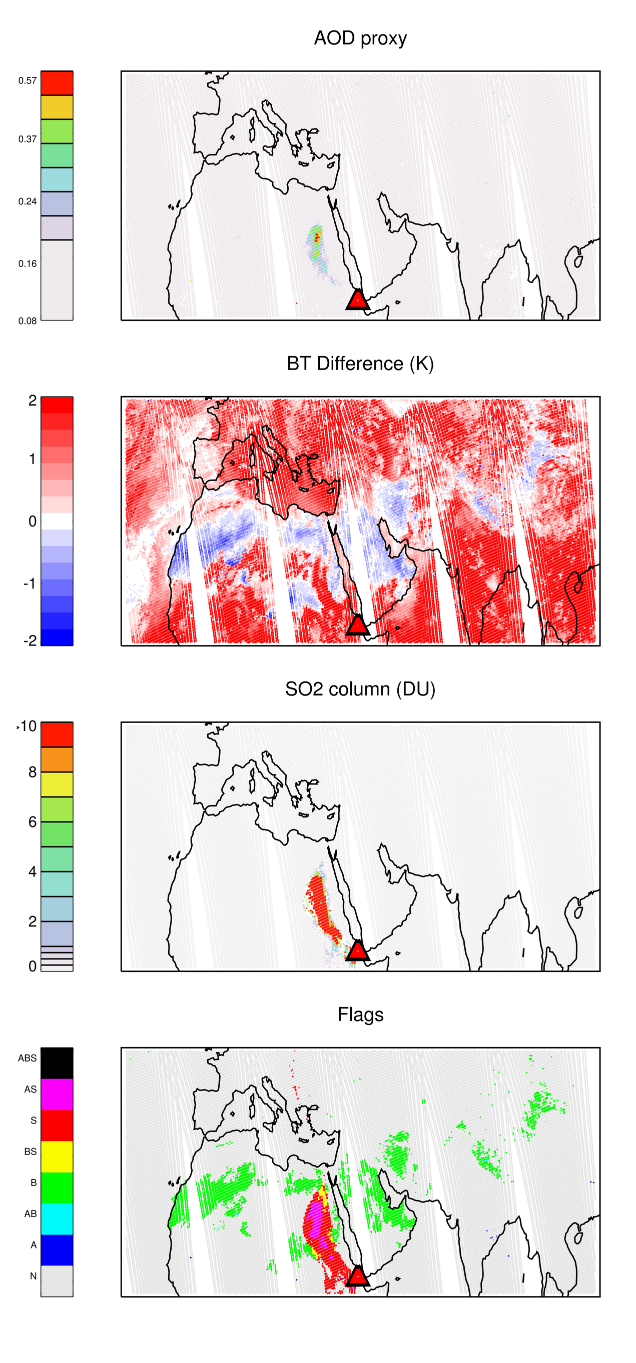

Fig. 4: IASI measurements from 13th June 2011, one day after the eruption of Nabro, Eritrea. Ash optical depth proxy, brightness temperature difference, SO_2 column concentration (see panel below) are shown along with a flag showing where the three methods have marked plumes: either aerosol (blue), BTD (green), or SO_2 (red).

Retrieving SO_2 with IASI

The SO_2 retrieval follows the method of Carboni et al. [2012] where the SO_2 concentration is parameterised as a gaussian profile in altitude. SO_2 column amount, height and thickness, and the surface skin temperature are estimated using optimal estimation [Rodgers, 2000]. Measurements from 1000–1200 cm^{-1} and 1300–1410 cm^{-1} (the SO_2 ν_1 and ν_3 bands) are used. The forward model is based on RTTOV [Saunders et al., 1999] extended to include SO_2. The SO_2 retrieval is not affected by underlying cloud (if the SO_2 is within or below an ash or cloud layer its signal will be masked and the retrieval will not work – this is indicated by a high retrieval cost).

Rigorous error propagation, including the incorporation of forward model and forward model parameter error, is built into the system, providing quality control and error estimates on the retrieved state. The altitude of the SO_2 plume strongly modulates the retrieval error as the contrast between plume temperature and surface temperature is a critical factor. Concentration error decreases with an increasing plume altitude. Typical uncertainties are 2 DU for a plume centred at 1.5 km and < 1 DU for plumes above 3 km.

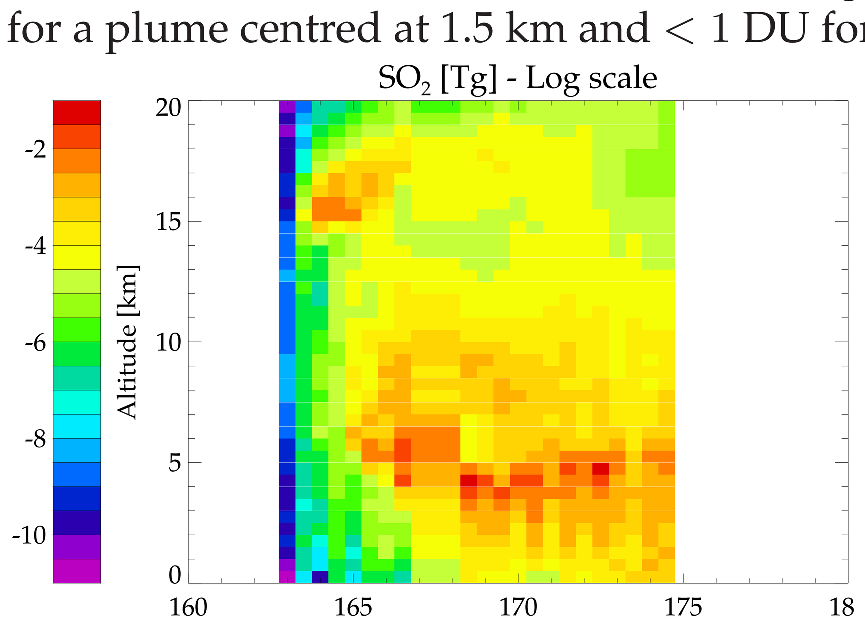

Fig. 5: SO_2 mass after the June 2011 eruption of Nabro, Eritrea. A plume is ejected into the stratosphere after the initial explosive eruption, followed by a period of degassing.

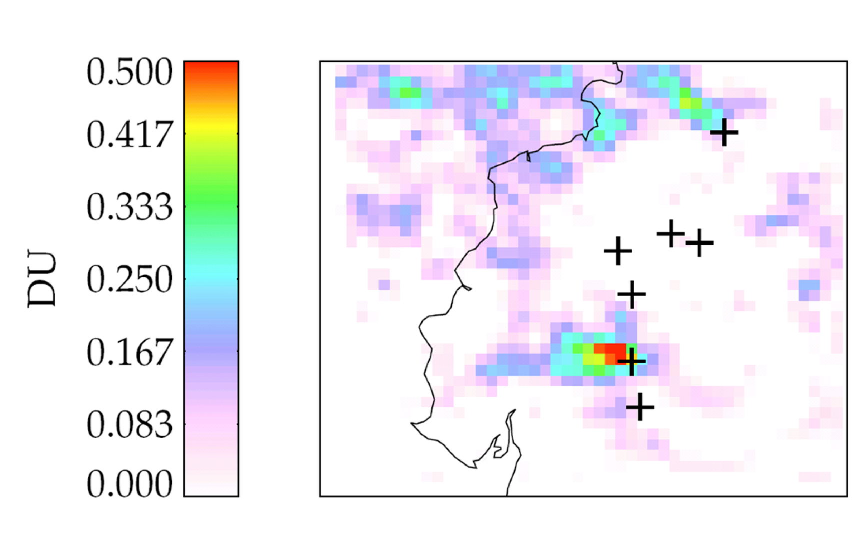

Fig. 6: Monthly mean retrieved SO_2 column amount over Equador. Active volcanoes are marked by (+). These signals are too weak to see in individual overpasses, but stand out over the noise in monthly average products.

SO_2 as a proxy for ash?

Given the potential complexities of retrieving ash, recent work was carried out to investigate using SO_2 flagging as a proxy for ash. In order to do this, the ash and SO_2 flags shown above were used to calculate a "missed ash fraction" (MAF), defined as the number of pixels flagged as ash, that were not also flagged as SO_2 (shown as blue in Fig. 7). For the case of the Puyehue-Cordòn Caulle eruption in June 2011, this initially meant a MAF of 30 %, rising with time as ash and SO_2 plumes separated (see Fig. 8). For the case of the 2010 eruption of Eyjafjallajökull (not shown) the initial eruption (in April) had MAF values between 40 and 90 % which are unacceptably high; the later ash ejections (in early May) had better values of below 30 %.

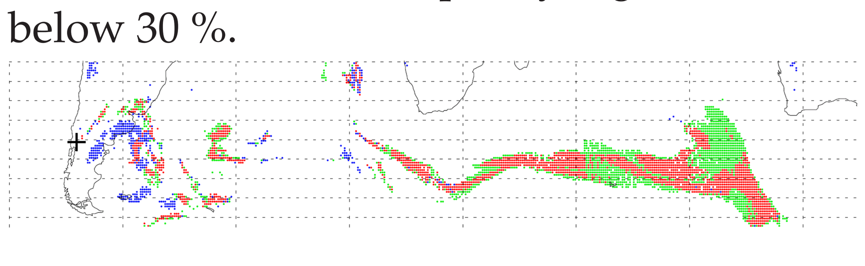

Fig. 7: Example flagging comparisons after the eruption of the Puyehue-Cordòn Caulle for 9th June 2011. The black cross marks the location of the volcano, coloured pixels indicate: **red:** both ash and SO_2 present; **green:** only SO_2 present; **blue:** only ash present.

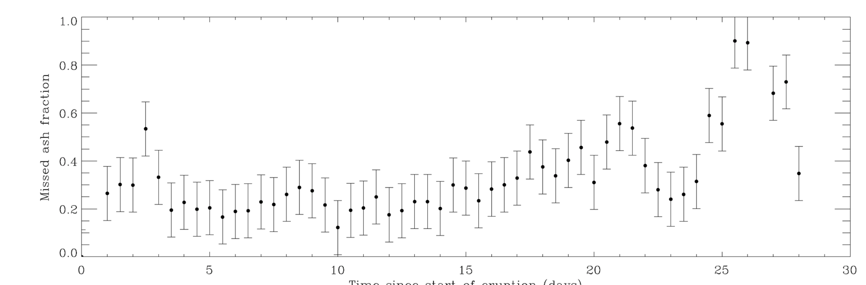

Fig. 8: Missed ash fraction as a function of time for the Puyehue eruption.

References

Carboni, E., R. G. Grainger, J. Walker, A. Dudhia, and R. Siddans, 2012. *Atmos. Chem. Phys.*, **12**(23):11417–11434, doi: 10.5194/acp-12-11417-2012.
Poulsen, C. A., R. Siddans, G. E. Thomas, A. M. Sayer, R. G. Grainger, et al., 2012. *Atmos. Meas. Tech.*, **5**(8):1889–1910, doi: 10.5194/amt-5-1889-2012.
Rodgers, C. D., 2000: *Inverse methods for atmospheric sounding: Theory and practice*. World Scientific Publishing Co.
Saunders, R. W., M. Matricardi, and P. Brunel, 1999. *Q. J. Roy. Meteor. Soc.*, **125**(556):1407–1425, doi: 10.1002/qj.1999.49712555615.
Thomas, G. E., S. F. Bass, R. G. Grainger, and A. Lambert, 2005. *App. Optics*, **44**(7):1332–1341, doi: 10.1364/AO.44.001332.
Walker, J., A. Dudhia, and E. Carboni, 2011. *Atmos. Meas. Tech.*, **4**(8):1567–1580, doi: 10.5194/amt-4-1567-2011.